

Quantification of (7*S*,8*R*)-Dihydroxy-(9*R*,10*S*)-epoxy-7,8,9,10-tetrahydrobenzo[*a*]pyrene Adducts in Human Serum Albumin by Laser-induced Fluorescence: Implications for the *in Vivo* Metabolism of Benzo[*a*]pyrene¹

Can C. Özbal, Paul L. Skipper, Mimi C. Yu, Stephanie J. London, Ramachandra R. Dasari, and Steven R. Tannenbaum²

Division of Bioengineering and Environmental Health [C. C. O., P. L. S., S. R. T.] and George R. Harrison Spectroscopy Laboratory [R. R. D.], Massachusetts Institute of Technology, Cambridge, Massachusetts 02139-4307; University of Southern California/Norris Comprehensive Cancer Center, University of Southern California, Los Angeles, California 90089-9176 [M. C. Y.]; and Epidemiology Branch, National Institute of Environmental Health Science, Research Triangle Park, North Carolina 27709 [S. J. L.]

Abstract

The ubiquitous environmental carcinogen benzo[*a*]pyrene (BaP) is metabolized *in vivo* in humans to its ultimate carcinogenic form of 7,8-dihydroxy-9,10-epoxy-7,8,9,10-tetrahydrobenzo[*a*]pyrene (BPDE). Mouse skin tumorigenicity studies indicate that the (7*R*,8*S*,9*S*,10*R*) enantiomer of BPDE, (7*R*,8*S*)-dihydroxy-(9*S*,10*R*)-epoxy-7,8,9,10-tetrahydrobenzo[*a*]pyrene [(7*R*,8*S*,9*S*,10*R*)-BPDE], is a potent tumor initiator, whereas the (7*S*,8*R*,9*R*,10*S*) enantiomer of BPDE, (7*S*,8*R*)-dihydroxy-(9*R*,10*S*)-epoxy-7,8,9,10-tetrahydrobenzo[*a*]pyrene [(7*S*,8*R*,9*R*,10*S*)-BPDE], may act as a tumor promoter. *In vitro* experiments have shown that human liver microsomes are capable of metabolizing BaP to both the (7*R*,8*S*,9*S*,10*R*) and (7*S*,8*R*,9*R*,10*S*) enantiomers of BPDE. However, the metabolism of BaP to (7*S*,8*R*,9*R*,10*S*)-BPDE has not been demonstrated in humans *in vivo*.

The adducts formed between human serum albumin (HSA) and the (7*S*,8*R*,9*R*,10*S*) and (7*R*,8*S*,9*S*,10*R*) enantiomers of BPDE have been described previously. (7*S*,8*R*,9*R*,10*S*)-BPDE forms a stable adduct at histidine¹⁴⁶ of HSA, whereas (7*R*,8*S*,9*R*,10*R*)-BPDE forms a relatively unstable ester adduct at aspartate¹⁸⁷ or glutamate¹⁸⁸ of HSA. Using high-performance liquid chromatography with laser-induced fluorescence (LIF) detector, we quantified the level of (7*S*,8*R*,9*R*,10*S*)-BPDE adducts at histidine¹⁴⁶ in HSA isolated from 63 healthy

males who were population control subjects for an ongoing case-control study of bladder cancer. By design, roughly half of the participants were lifelong nonsmokers ($n = 35$), whereas the remaining 28 participants were current smokers of varying intensities. HP-BPDE adducts were detected in 60 of the 63 samples (95%) by HPLC-LIF. Adduct levels ranged from undetectable (<0.04 fmol/mg HSA) to 0.77 fmol/mg HSA. The samples had a mean and median (7*S*,8*R*,9*R*,10*S*)-BPDE-HSA adduct level of 0.22 and 0.16 fmol of adduct/mg albumin, respectively. Mean adduct levels did not differ between smokers and nonsmokers ($P = 0.72$). Occupational exposure to polycyclic aromatic hydrocarbons was unrelated to adduct level ($P = 0.62$). Intake frequencies of two food items showed statistically significant associations with adduct levels. Consumption of sweet potatoes was negatively related to adduct level ($P = 0.029$), whereas intake of grapefruit juice was positively related to adduct level ($P = 0.045$). None of the three indices of residential ambient air pollution under study showed a statistically significant association with adduct levels.

Introduction

The metabolic activation of BaP³ has been extensively studied and is well understood (reviewed in Ref. 1). The major metabolic sequence involves initial epoxidation of BaP by cytochrome P-450 1A1 to BaP-7,8-oxide. Hydrolysis of BaP-7,8-oxide to the BaP-7,8-dihydrodiol is catalyzed by epoxide hydrolase. Recently, cytochrome P-450 1B1 has also been shown to be capable of metabolizing BaP to BaP-7,8-dihydrodiol in the presence of epoxide hydrolase (2). BaP-7,8-dihydrodiol is further metabolized to BPDE by cytochrome P450 3A4 or prostaglandin H synthase. BPDE is resistant to hydrolysis by epoxide hydrolase because of the steric hindrance of the diol and may react with nucleophilic centers in DNA or proteins.

Epoxidation at the 9,10 position of (7*S*,8*S*)-dihydroxy-7,8-dihydrobenzo[*a*]pyrene yields the (7*S*,8*R*,9*R*,10*S*)-BPDE enantiomer, whereas epoxidation at the 9,10 position of (7*R*,8*R*)-

Received 12/28/99; revised 4/12/00; accepted 5/9/00.

The costs of publication of this article were defrayed in part by the payment of page charges. This article must therefore be hereby marked *advertisement* in accordance with 18 U.S.C. Section 1734 solely to indicate this fact.

¹ This work was supported by National Institute of Environmental Health Sciences Grants P01 ES05622 (to Massachusetts Institute of Technology) and P30 ES07048 (to University of Southern California), and National Cancer Institute Grants R35 CA53890 and R01 CA65726 (to University of Southern California).

² To whom requests for reprints should be addressed, at Massachusetts Institute of Technology, Building 56-731, 77 Massachusetts Avenue, Cambridge, MA 02139-4307.

³ The abbreviations used are: BaP, benzo[*a*]pyrene; BPDE, 7,8-dihydroxy-9,10-epoxy-7,8,9,10-tetrahydrobenzo[*a*]pyrene; (7*R*,8*S*,9*S*,10*R*)-BPDE, 7*R*,8*S*-dihydroxy-9*S*,10*R*-epoxy-7,8,9,10-tetrahydrobenzo[*a*]pyrene; (7*S*,8*R*,9*R*,10*S*)-BPDE, 7*S*,8*R*-dihydroxy-9*R*,10*S*-epoxy-7,8,9,10-tetrahydrobenzo[*a*]pyrene; HSA, human serum albumin; 3-MC, 3-methylcholanthrene; BPT, 7,8,9,10-tetrahydroxy-7,8,9,10-tetrahydrobenzo[*a*]pyrene; LIF, laser-induced fluorescence; HP, histidine¹⁴⁷-proline¹⁴⁸; HPY, histidine¹⁴⁶-proline¹⁴⁷-tyrosine¹⁴⁸; N^π-H-BPDE, N^π-(7*S*,8*R*,9*R*-trihydroxy-7,8,9,10-tetrahydro-benzo[*a*]pyren-10*R*-yl)histidine; HPLC, high-performance liquid chromatography; PMT, photomultiplier tube; PAH, polycyclic aromatic hydrocarbon.

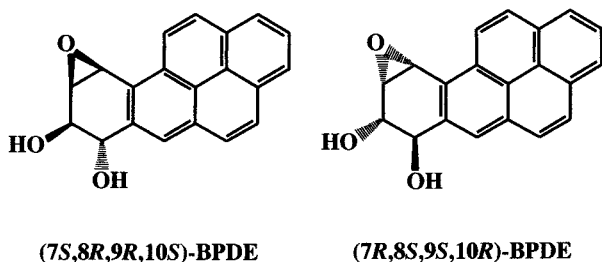


Fig. 1. Structures of the (7S,8R,9R,10S) and (7R,8S,9S,10R) enantiomers of BPDE.

dihydroxy-7,8-dihydrobenzo[a]pyrene yields the (7R,8S,9S,10R)-BPDE enantiomer (3). The structures of (7S,8R,9R,10S)-BPDE and (7R,8S,9S,10R)-BPDE are shown in Fig. 1. These two enantiomers of BPDE have markedly different carcinogenic potencies in rodent assays (1).

An assay commonly used to determine the tumorigenic potency of possible carcinogens is the multistage carcinogenesis model in mouse skin. In this assay, the induction of skin tumors in mice is accomplished by a multistage process involving initiation and promotion (reviewed in Ref. 4). Initiation is typically accomplished by the topical application of a single dose of a carcinogen, followed by repeated topical applications of a tumor promoter such as 12-*O*-tetradecanoylphorbol-13-acetate. Tumor promoters allow for clonal expansion of an initiated cell by promoting cell division. Visible tumors typically appear as the result of prolonged treatment with a tumor promoter unless the initiating compound is a complete carcinogen. Complete carcinogens do not require the application of promoters to induce tumors on mouse skin.

The relative tumorigenicity of the four optical isomers of BPDE was tested on female CD-1 and Sencar mice (5). Initiation with isomers of BPDE was followed with twice weekly applications of 12-*O*-tetradecanoylphorbol-13-acetate for 24 weeks. The only enantiomer of BPDE with significant tumor-initiating activity was found to be (7R,8S,9S,10R)-BPDE.

The ability of (7R,8S,9S,10R)-BPDE to initiate tumors was further demonstrated in the newborn mouse adenoma assay. Of the four isomers of BPDE, (7R,8S,9S,10R)-BPDE was the most potent in inducing lung adenomas in newborn mice (6). Because rapid cellular division takes place as the mice are growing, treatment with tumor promoters is not necessary for the induction of tumors when compounds with tumor-initiating activity are tested in the newborn mouse adenoma assay.

BaP and 7,8-dihydroxy-7,8-dihydrobenzo[a]pyrene are complete carcinogens and do not require the repeated application of a promoter to induce tumors (7). Repeated topical applications of BaP or racemic (7S,8S) and (7R,8R)-dihydroxy-7,8-dihydrobenzo[a]pyrene was strongly tumorigenic in mice (8). Repeated topical application of racemic (7R,8S,9S,10R)- and (7S,8R,9R,10S)-BPDE on mouse skin was very effective in causing hyperplasia in C57BL/6J mice (9). Surprisingly, these hyperplastic lesions did not develop into tumors with repeated topical exposure (10, 11). It has been suggested that the inability of BPDE to induce tumors on mouse skin without the application of a tumor promoter may be because of poor penetration into skin cells attributable to the extreme instability, high reactivity, and/or high polarity of these molecules (5). This hypothesis is supported by the observation that benzo[a]pyrene-7,8-oxide was very weakly carcinogenic on mouse

skin as compared with BaP and 7,8-dihydroxy-7,8-dihydrobenzo[a]pyrene (8).

Given that (7R,8S,9S,10R)-BPDE is a potent tumor initiator in the mouse skin tumorigenicity assay and the newborn mouse adenoma assay and that racemic (7R,8S,9S,10R)- and (7S,8R,9R,10S)-BPDE is a powerful inducer of hyperplasia in mouse skin, it has been suggested that (7R,8S,9S,10R)- and (7S,8R,9R,10S)-BPDE can act together as a complete carcinogen.⁴

When activated with 3-MC rat liver microsomes, BaP was almost exclusively (98%) metabolized to (7R,8R)-dihydroxy-7,8-dihydro-BaP (12). Unlike 3-MC-activated rat liver microsomes, human liver microsomes produce a mixture of (7-*R*, 8-*R*)-dihydroxy-7,8-dihydroBaP and (7S,8S)-dihydroxy-7,8-dihydroBaP. The amount of (7S,8S)-dihydroxy-7,8-dihydroBaP formed upon metabolic activation of BaP by human liver microsomes *in vitro* ranged from 28 to 56% (13). The metabolism of BaP by human skin in short-term organ culture also was investigated (14). A mixture of (7R,8R)- and (7S,8S)-dihydroxy-7,8-dihydro-BaP metabolites were detected. These results show that BaP is metabolized to both (7R,8R)- and (7S,8S)-dihydroxy-7,8-dihydro-BaP *in vitro*. (7R,8R)- and (7S,8S)-dihydroxy-7,8-dihydro-BaP are further metabolized to (7R,8S,9S,10R)- and (7S,8R,9R,10S)-BPDE, respectively. However, the presence of (7S,8R,9R,10S)-BPDE has not been shown in humans *in vivo*.

The major HSA adducts of the (7R,8S,9S,10R) and (7S,8R,9R,10S) enantiomers of BPDE have been fully characterized by fluorescence line-narrowing spectroscopy (15) and mass spectrometry (16–18). These studies showed that the major stable adduct of a racemic mixture of the (7R,8S,9S,10R) and (7S,8R,9R,10S) enantiomers of BPDE in HSA was at histidine¹⁴⁶ and that this adduct was formed specifically by the (7S,8R,9R,10S) enantiomer. (7R,8S,9S,10R)-BPDE forms a relatively unstable ester adduct with HSA as aspartate¹⁸⁷ or glutamate¹⁸⁸ (18). The (7S,8R,9R,10S) enantiomer of BPDE has been shown to form an adduct exclusively at the *N*⁷-position of the imidazole ring of histidine¹⁴⁶ in HSA (18).

Gas chromatography/mass spectroscopy-based methods for the quantification of BPT released from proteins after acid hydrolysis have been developed (19, 20). With this approach, BPDE-HSA adducts were quantified in 44 individuals with detectable adducts in 24 cases (57%; median, 0.11 fmol BPT/mg HSA; Ref. 21). The acid hydrolysis step used in the method was effective in converting ester adducts, such as those formed between (7R,8S,9S,10R)-BPDE and aspartate¹⁸⁷ or glutamate¹⁸⁸ of HSA, into BPT. However, more stable adducts, such as those formed between (7S,8R,9R,10S)-BPDE and histidine¹⁴⁶ of HSA, were not hydrolyzed by acidic conditions and cannot be detected by this method (data not shown).

In this study, we have investigated the occurrence of HSA adducts of (7S,8R,9R,10S)-BPDE in a population of healthy human volunteers using a LIF-based method for the detection of (7S,8R,9R,10S)-BPDE adducts at histidine¹⁴⁶ in HSA. Widespread occurrence of this adduct was observed, indicating that the formation of (7S,8R,9R,10S)-BPDE is a significant pathway in the metabolism of BaP in humans. The presence of both the (7R,8S,9S,10R) and (7S,8R,9R,10S) enantiomers of BPDE *in vivo* in humans and the possibility that this enantiomeric pair can act as a complete carcinogen has important implications for human carcinogenesis.

⁴ T. J. Slaga, personal communication.

Materials and Methods

Chemicals. BPDE was purchased from the National Cancer Institute Chemical Repository maintained by ChemSyn Science Laboratories (Lenexa, KS). HSA (fatty acid-free) and L-histidine monohydrochloride monohydrate were purchased from Sigma-Aldrich (St. Louis, MO). Pronase (nuclease-free, from *Streptomyces griseus*) was purchased from CalBiochem (San Diego, CA). Dichlorodimethylsilane used in the silanization of glassware was purchased from Supelco (Bellefonte, PA). All other chemicals used were of analytical grade.

Synthetic BPDE-HSA and N⁷-H-BPDE Standards. Synthetic BPDE-HSA adduct was prepared as described previously (16). Enzymatic digestion of mg quantities of racemic (7R,8S,9S,10R)- and (7S,8R,9R,10S)-BPDE adducted HSA with Pronase (10% w/w; 37°C for 24 h) yielded a mixture of two major adducted peptides identified previously as (7S,8R,9R,10S)-BPDE adducted HP and HPY (16). Digestion proceeded to completion in samples with subpicomolar adduct levels, yielding only the HP-BPDE adduct. The synthesis of N⁷-(7,8,9-trihydroxy-*r-r*-7,*t*-8,*t*-9,*c*-10-tetrahydrobenzo[*a*]pyren-10-yl)histidines for use as the internal standard was performed as described previously with minor modifications (16). The final purification of the N⁷-H-BPDE adduct was done by sequential C18 and C4 reversed phase HPLC.

Study Subjects. HP-BPDE adducts were measured on plasma samples collected from 63 male residents of Los Angeles County, CA. These healthy men were neighborhood-, age-, and sex-matched control subjects for an ongoing case-control study of bladder cancer in Los Angeles. The mean age of subjects was 56.5 years (range, 36–70 years). By design, approximately half ($n = 35$) of the subjects were lifelong nonsmokers, whereas the remaining 28 subjects were current smokers of various intensities at the time of blood collection.

As part of the case-control study of bladder cancer, each subject was administered a structured questionnaire at the time of recruitment. Solicited information included lifetime history of tobacco use, lifetime occupational history, and dietary habits ~2–5 years ago. The dietary section of the questionnaire was designed to assess primarily exposure to dietary nitrosamines, vitamins A and C, and various carotenoids. Subjects were asked to provide the usual intake frequencies of 40 food groups, which included a variety of fruit and vegetables that are rich in carotenoids and vitamins A and C, and different types of cured meats (such as fried bacon/ham, hot dogs, and others), which contain nitrosamines and their precursors.⁵ To assess possible association between HP-BPDE adduct level and occupational exposure to PAHs, an occupational medicine physician (S. J. L.) blindly (*i.e.*, without knowledge of subject's adduct level) reviewed the current occupations of study subjects and classified them into one of three possible categories: 0, definitely not exposed; 1, possibly exposed; and 2, likely to be exposed. Occupational information included complete job title, usual activities and duties, type of business or industry, and the name of the company.

We also were interested in relating HP-BPDE adduct levels in study subjects to general air quality levels in their neighborhoods of residence. There is no routine air monitoring of PAHs. However, the Southern California Air Quality Control Board provides daily measurements of the criteria air

pollutants, particulates (PM10), nitrogen oxide, and ozone by zip code for the entire Los Angeles County. Because vehicular and industrial emissions are the major sources of both of these criteria, air pollutants and PAHs (22), we used these routinely measured pollutants as surrogates for ambient PAHs. Using the residential zip codes of study subjects, levels of ambient air pollution representing the average 24-h concentrations over a 2-month period (month of blood draw plus the previous month) were computed for all subjects.

Isolation of HSA from Plasma. Plasma samples collected from study subjects had been continuously frozen at –20°C until analysis. Blinded samples were shipped on dry ice from Los Angeles to the Massachusetts Institute of Technology, where they were thawed, and aliquots (50–200 μ l) were diluted with an equal amount of PBS (1 \times , pH 7.4). Total plasma proteins were precipitated with the addition of saturated (NH₄)₂SO₄ (80% v/v) and cooled at 4°C for a minimum of 2 h. The precipitated plasma proteins were centrifuged at 9000 $\times g$ for 15 min, and the supernatant was decanted. The plasma proteins were redissolved in PBS and dialyzed against PBS at 4°C in 10,000 molecular weight cutoff membranes with one change of dialysis buffer. After dialysis, samples were transferred to silanized vials with Teflon-lined caps.

No further purification of the albumin was undertaken because the method quantifies the BPDE-adducted dipeptide HP, and it is extremely unlikely that the same dipeptide adduct would form in a different protein. The volume of each sample after dialysis was recorded, and the protein concentration was determined on an aliquot using the Pierce BCA protein assay (Pierce Corp., Rockford, IL).

Isolation and Purification of HP-BPDE. Isolated and quantified plasma proteins were enzymatically digested with Pronase to yield (7S,8R,9R,10S)-BPDE adducted HP as described (16). This adduct was purified by immunoaffinity chromatography using a monoclonal antibody (8E11-raised against the guanoside adduct of BPDE; a generous gift from Dr. R. Santella, Columbia University, New York, NY; Ref. 23) covalently linked to CNBr-activated Sepharose 4B (Sigma Chemical Co., St. Louis, MO). Prior to immunoaffinity chromatography, N⁷-H-BPDE (4.0 fmol) was added to each digested HSA sample as an internal standard. The immunoaffinity chromatography was performed in a custom-fabricated microcolumn, which was prepared by forming a porous silica frit at the tip of a glass Pasteur pipette. The frit was made as described previously (24), and the entire microcolumn was silanized. A total of 15 μ l of 8E11 antibody gel (150 μ g of 8E11) was added to the standard spiked samples, and the mixture was rotated at 4°C for 16 h. The sample-antibody mixture was loaded into the microcolumns, and a gentle vacuum was applied to draw the liquid through. The antibody gel was washed with PBS (6 \times 200 μ l), and BPDE adducts were eluted with 30 μ l of CH₃OH and collected in a silanized conical vial. Samples were evaporated to dryness with a stream of grade 5.0 He purified with an activated charcoal filter (Hewlett-Packard) and redissolved in H₂O distilled from KMnO₄ (20 μ l) prior to analysis by HPLC-LIF.

HPLC-LIF Instrument. The output of an HPLC pump (Hewlett-Packard model 1050) operating at 0.4 ml/min was passed through a flow splitter (LC Packings model AcuRate IC 400 VAR) to provide accurate gradients at flow rates of 5 μ l/min. Samples were loaded onto the column using an injector (Rheodyne model 7125) with a 5- μ l sample loop. HPLC columns were manufactured in-house from a length of fused silica tubing (320 μ m internal diameter \times 450 μ m outer diameter;

⁵ J. E. Castelao, J.-M. Yuan, M. Gago-Dominguez, J. H. Hankin, R. K. Ross, and M. C. Yu. Vitamin C and carotenoids protect against smoking-related bladder cancer, submitted for publication.

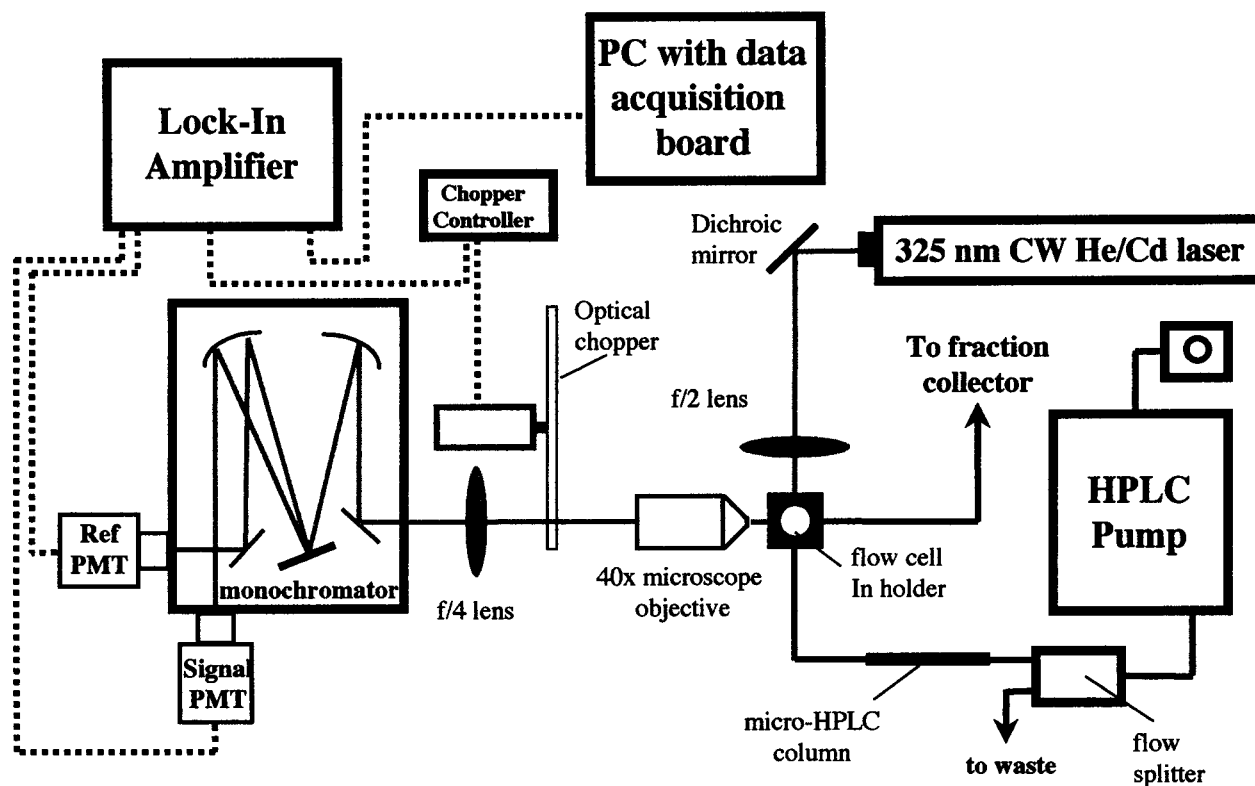


Fig. 2. Schematic outline of the HPLC-LIF instrument.

Polymicro Technologies) that had a semiporous frit at the end. The frit was manufactured as described previously (24). Columns were packed with Poros 10R2 (PerSeptive Biosystems, Framingham, MA), a polymeric packing material with C18-like characteristics. The HPLC eluent was passed through a length of 75- μm internal diameter fused silica capillary (230 μm , outer diameter) with a laser illumination window, immobilized in a custom-built mount.

A 30 mW CW helium-cadmium laser (Liconix), operating at the 325 nm line, was used to irradiate the HPLC eluent. The laser light was filtered by a 350-nm short-pass filter and focused onto the fused silica capillary with an $f/2$ lens. The fluorescence emission was collected at right angles with a $\times 40$ microscope objective and focused onto the entrance slit of a modified 0.22-m monochromator (Spex model 1681) with f -matching optics. All optical components in the instrument were mounted on micrometers to facilitate the alignment of the laser beam and collection optics. The monochromator was modified for simultaneous transmission of two wavelengths 50 nm apart. Fluorescence was detected by two photomultiplier tubes (PMT; Hamamatsu R-928). One PMT monitored the fluorescence intensity of the sample at 400 nm, whereas the second acted as a reference by monitoring the fluorescence at 450 nm. The background fluorescence was continuously subtracted from the sample fluorescence. The PMT outputs were subtracted and amplified by a lock-in amplifier equipped with an optical chopper (SciTec Instruments model MC500, Cornwall, United Kingdom), and the signal was digitized with a data acquisition board (National Instruments model AT-MIO-16E, Austin, TX) and monitored on a PC with appropriate software (National Instru-

ments DaqWare). A diagram of the HPLC-LIF instrument is shown in Fig. 2.

Statistical Analysis. The distribution of the HP-BPDE adducts in study subjects was markedly skewed; therefore, formal statistical testings were performed on logarithmically transformed values, and geometric (as opposed to arithmetic) mean values are presented. We used the ANOVA method to compare log adduct values by levels of current smoking habits, dietary intake frequencies of various food groups, and occupational exposure to PAH (25). To examine the relationship between indices of residential ambient air pollution and HP-BPDE adducts, Pearson product-moment correlation coefficients and their corresponding P s were computed between log values of adducts and log values of air pollutants (25). Two-sided P s that were $<5\%$ were considered statistically significant. All P s quoted are 2-sided.

Results

HPLC-LIF Method. The detection limit of the HPLC-LIF instrument for synthetically prepared HP-BPDE standard was 0.01 fmol. The detection limit of the method for HP-BPDE adducts isolated from HSA samples was 0.04 fmol/mg of HSA because of increased background levels in human samples. The dose response of the HPLC-LIF instrument was shown to be linear up to 0.62 fmol of HP-BPDE adduct, which was the highest concentration measured. The areas of the HP-BPDE and N^{π} -H-BPDE internal standard fluorescence peaks were determined, and the amount of HP-BPDE adduct was calculated from the ratio of the HP-BPDE adduct and the N^{π} -H-

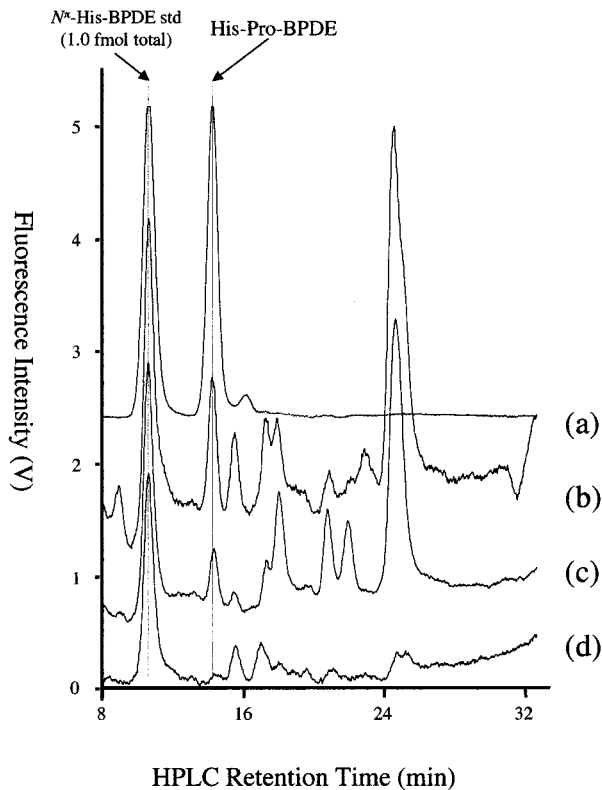


Fig. 3. Comparison of three HSA samples with synthetic standards prepared and analyzed as described. A 1.0 fmol total injection of synthetically prepared N^{π} -H-BPDE and HP-BPDE standard (a) is compared with sample 31141 (b), which had 0.35 fmol (7*S*,8*R*,9*R*,10*S*)-BPDE adducts/mg of serum albumin; sample 31050 (c), which had 0.14 fmol (7*S*,8*R*,9*R*,10*S*)-BPDE adducts/mg of serum albumin; and sample 32833 (d), which had an undetectable level of (7*S*,8*R*,9*R*,10*S*)-BPDE serum albumin adducts.

BPDE internal standard peak areas. The fluorescence quantum yields of HP-BPDE and N^{π} -H-BPDE were shown to be within 10% of one another. To determine the coefficient of variability of the method, 10 200- μ l aliquots of a 2-ml plasma sample were independently isolated, purified, and analyzed by HPLC-LIF. The coefficient of variability of the method was 22%.

The (7*S*,8*R*,9*R*,10*S*)-BPDE-HSA adduct peak was identified in human plasma samples by comigration in both C18 and C4 reverse phase HPLC systems with a synthetically prepared standard of the N^{π} -(7*S*,8*R*,9*R*-trihydroxy-7,8,9,10-tetrahydrobenzo[*a*]pyren-10*R*-yl) derivative of the dipeptide histidine-proline. Coinjection of selected serum albumin digests isolated from human plasma with synthetically prepared HP-BPDE resulted in a single sharp HPLC-LIF peak (data not shown). Typical HPLC-LIF chromatograms and synthetically prepared N^{π} -H-BPDE and HP-BPDE standards are shown in Fig. 3.

(7*S*,8*R*,9*R*,10*S*)-BPDE Adduct Analysis in HSA Samples. The 63 HSA samples isolated from plasma collected from healthy male residents of Los Angeles County, CA, were analyzed. HP-BPDE adducts were detected in 60 of the 63 samples (95%) by HPLC-LIF. A comparative illustration of HPLC-LIF results from three plasma samples is shown in Fig. 3. Adduct levels ranged from undetectable (<0.04 fmol/mg HSA) to 0.77 fmol/mg HSA. The samples had a mean and median (7*S*,8*R*,9*R*,10*S*)-BPDE-HSA adduct level of 0.22 and 0.16 fmol of adduct/mg albumin, respectively. A frequency distribution of

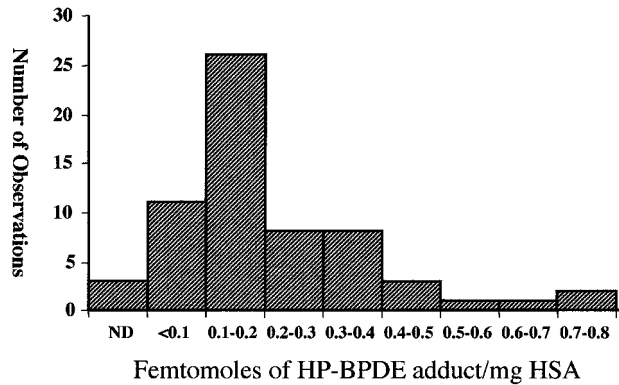


Fig. 4. Levels of (7*S*,8*R*,9*R*,10*S*)-BPDE adducts at the N^{π} position of the imidazole ring of histidine¹⁴⁶ in HSA isolated from 63 healthy men from Los Angeles County, CA.

the (7*S*,8*R*,9*R*,10*S*)-BPDE-HSA adduct levels in the 63 samples analyzed is shown in Fig. 4.

Adduct levels did not differ between smokers and non-smokers ($P = 0.72$), although a mean level in smokers was modestly elevated relative to nonsmokers (172.2 versus 160.3 fmol/mg HSA). There was no association between adduct level and number of cigarettes smoked per day ($P = 0.54$).

We compared adduct levels between weekly (*i.e.*, at least once a week), monthly (once a month to less than weekly), and less frequent consumers of each of 40 food groups listed in the Bladder Cancer Study questionnaire (see "Materials and Methods"). We noted two statistically significant associations between dietary frequencies and adduct levels. There was a negative association between intake of sweet potatoes and HP-BPDE adducts ($P = 0.029$). Mean adduct level in the 45 subjects who consumed sweet potatoes less than monthly was 182.5 fmol/mg HSA. The corresponding mean adduct values in monthly ($n = 15$) and weekly ($n = 3$) consumers were 148.3 and 66.0 fmol/mg HSA, respectively. Intake of grapefruit juice, on the other hand, was positively associated with HP-BPDE adducts ($P = 0.045$). Mean adduct levels in the 42 subjects who drank the juice less than monthly was 149.9 fmol/mg HSA. The corresponding mean adduct values in monthly ($n = 9$) and weekly ($n = 12$) consumers were 150.5 and 250.9 fmol/mg HSA, respectively.

Among the 63 subjects, three were considered likely to be exposed to PAH on the job, six were possibly exposed on the job, and the remaining 54 subjects were definitely not exposed occupationally. We found no difference in mean adduct levels between groups 1 and 2 versus 3 ($P = 0.62$).

We examined three indices of residential ambient air pollution (particulates, nitrogen oxide, and ozone) in relation to HP-BPDE adducts among the 63 study subjects. None of the correlation coefficients reached statistical significance (particulates, $r = 0.03$, $P = 0.80$; nitrogen oxide, $r = 0.13$, $P = 0.32$; ozone, $r = -0.11$, $P = 0.39$).

Discussion

The strong activity of the (7*R*,8*S*,9*S*,10*R*) isomer of BPDE in rodent mutagenicity and carcinogenicity assays, along with the observation that (7*R*,8*S*,9*S*,10*R*)-BPDE is the major diol epoxide product of the metabolism of BaP by 3-MC-activated rat liver microsomes, has led to the hypothesis that (7*R*,8*S*,9*S*,10*R*)-BPDE is the principal BPDE stereoisomer of biological impor-

tance. However, other isomers of BPDE are not devoid of biological activity. It has been shown that BaP is metabolized to both the (7R,8S,9S,10R) and (7S,8R,9R,10S) enantiomers of BPDE by human liver microsomes (13). Furthermore, there is evidence that this enantiomeric pair of BPDE may act as a complete carcinogen with (7R,8S,9S,10R)-BPDE acting as the tumor initiator (5, 6) and (7S,8R,9R,10S)-BPDE acting as the tumor promoter by inducing hyperplasia (9).

We have developed a method for the direct detection of stable adducts of (7S,8R,9R,10S)-BPDE at histidine¹⁴⁶ in HSA. The method involves the quantification of fluorescence from the adduct in an HPLC-LIF instrument. Identification of the peak observed in the HPLC-LIF chromatograms of HSA samples depended on chromatographic retention time. Confirmation of the identity of the fluorescence peak seen in HSA samples was provided by coinjection analysis with synthetically prepared HP-BPDE adduct in both C18 and C4 reversed phase systems (data not shown), by the fact that the compound has fluorescence emission at 400 nm upon excitation at 325 nm, and by the fact that the compound was retained by the 8E11 immunoaffinity column. Further spectroscopic characterization of the compound was not possible in these experiments because of the extremely low level of adducts. However, the presence of HP-BPDE adducts in Pronase digests of larger amounts of HSA isolated from human plasma has been demonstrated previously by HPLC with tandem mass spectrometry (26). HPLC-LIF chromatograms of digested HSA isolated from human plasma revealed the presence of other fluorescent compounds. The retention of these inherently fluorescent compounds by the 8E11 immunoaffinity column suggests that they may be peptide adducts of other PAHs. Although structural characterization is not possible at the subfemtomolar level, isolation and identification of these peaks in larger samples of HSA is a future goal of this research.

The detection of BPDE adducts at histidine¹⁴⁶ in HSA reveals the metabolic formation of (7S,8R,9R,10S)-BPDE in humans *in vivo* from BaP because it has been demonstrated previously that the histidine¹⁴⁶ adduct is formed only by the (7S,8R,9R,10S) of BPDE (18). The major HSA adduct of the (7R,8S,9S,10R)-BPDE is an acid hydrolyzable ester at aspartate¹⁸⁷ or glutamate¹⁸⁸ (18). Using a different analytical method, Pastorelli *et al.* (19) hydrolyzed BPDE adducts in HSA to BPT by heating the samples at 80°C for 60 min in 0.3 N hydrochloric acid. Although this procedure quantitatively hydrolyzes the ester adduct formed by (7R,8S,9S,10R)-BPDE at aspartate¹⁸⁷ or glutamate¹⁸⁸ to BPT, we have demonstrated that the (7S,8R,9R,10S)-BPDE adduct at histidine¹⁴⁶ is stable under these conditions and is not hydrolyzed (data not shown). It may thus be inferred that the method of Pastorelli *et al.* (19) detects adducts of (7R,8S,9S,10R)-BPDE. Therefore, the two methods are selective for adducts of (7R,8S,9S,10R)-BPDE and (7S,8R,9R,10S)-BPDE in HSA.

Our results indicate that BaP is metabolized to (7S,8R,9R,10S)-BPDE in humans *in vivo*, with the resultant formation of stable adducts with HSA at histidine¹⁴⁶. The results of Pastorelli *et al.* (21) indicate the formation of (7R,8S,9S,10R)-BPDE as well as its corresponding HSA adduct. The median adduct level of 0.16 fmol of (7S,8R,9R,10S)-BPDE adducts/mg of HSA determined in this study is comparable with the median adduct level of 0.11 fmol of (7R,8S,9S,10R)-BPDE adducts/mg of HSA reported by Pastorelli *et al.* (21).

We have conducted a preliminary investigation of BPDE adducts in HSA in relation to cigarette smoking, occupational exposure to PAHs, dietary habits, and residential ambient air

pollution. We found no difference in HP-BPDE adduct levels between smokers and nonsmokers. These findings are compatible with prior studies noting a lack of association between cigarette smoking status and level of PAH-DNA adducts in WBCs (27). In contrast, studies examining PAH-DNA adduct level in lung bronchial epithelial cells have consistently found higher adduct levels in smokers relative to nonsmokers (27, 28).

In our exploratory investigation of dietary factors and HP-BPDE adduct levels, we noted statistically significant associations between adducts and intake of sweet potatoes (lower adducts in more frequent consumers) and grapefruit juice (higher adducts in more frequent consumers). These could be indirect associations, merely reflecting the correlations between intake of sweet potatoes/grapefruit juice with BPDE-associated dietary factors. Alternatively, these two food items may exert a direct effect on BPDE adducts. It is interesting to note that water extracts of sweet potatoes effectively decreased the level of BaP-induced mutagenicity in *Salmonella typhimurium* (29). In rats, multiple doses of grapefruit juice (0.2 ml/day for 10 days) led to increased overall mixed function oxidase activity in the liver (30). The effect of prolonged exposure to grapefruit juice in liver enzymes in humans is unknown. If the murine model is applicable to humans, their increased hepatic mixed function oxidase activity as a result of frequent grapefruit juice intake may offer an explanation for the increased BPDE-HSA adducts in this subgroup of individuals.

We did not observe any association between BPDE-HSA adduct level and occupational exposure to PAH or residential ambient air pollution. Our very small sample size precludes any firm conclusion from these negative findings. In addition, our exposure measures were rather crude, thus limiting our ability to detect correlations. For occupational exposure, we only had self-reported job title and industry of employment available to us. For residential ambient air pollution, because ambient PAHs are not measured routinely in Los Angeles, we used measurements of other air pollutants, PM10, nitrogen oxide, and ozone, that are also largely derived from vehicular and industrial combustion. Furthermore, although vehicular emissions have been found to be an important source of indoor PAH exposure, there are other indoor sources of PAHs, such as environmental tobacco smoke and cooking, that are not captured by these ambient measurements (31).

A quantitative comparison of HSA adducts formed by the (7R,8S,9S,10R) and (7S,8R,9R,10S) enantiomers of BPDE in the same individual is a future goal of this research. Such a comparison could be useful both as a biomarker of BaP exposure and as a noninvasive method to assay the relative activity of cytochrome P-450 enzymes in humans. Noninvasive experiments can be designed in which the effects of cytochrome P-450 inhibiting or inducing compounds can be monitored by determining their effects on the metabolism of BaP to the (7R,8S,9S,10R) or (7S,8R,9R,10S) enantiomer of BPDE. The relative levels of (7R,8S,9S,10R) and (7S,8R,9R,10S) enantiomers of BPDE can be monitored through the independent quantification of HSA adducts of each enantiomer.

Acknowledgments

We thank Susan Roberts and Kazuko Arakawa of the University of Southern California/Norris Comprehensive Cancer Center for assistance in data collection and management. In addition, we thank Richard Reiss of Sonoma Technologies, Santa Rosa, CA, for providing the air pollution data.

References

1. Conney, A. H., Chang, R. L., Jerina, D. M., and Wei, S.-J. C. Studies on the metabolism of benzo[a]pyrene and dose-dependent differences in the mutagenic

- profile of its ultimate carcinogenic metabolite. *Drug Metab. Rev.*, *26*: 125–163, 1994.
2. Shimada, T., Gillam, E. M. J., Oda, Y., Tsumura, F., Sutter, T. R., Guengerich, F. P., and Inoue, K. Metabolism of benzo[*a*]pyrene to *trans*-7,8-dihydroxy-7,8-dihydrobenzo[*a*]pyrene by recombinant human cytochrome P450 1B1 and purified liver epoxide hydrolase. *Chem. Res. Toxicol.*, *12*: 623–629, 1999.
 3. Wood, A. W., Chang, R. L., Levin, W., Yagi, H., Thakker, D. R., Jerina, D. M., and Conney, A. H. Differences in the mutagenicity of the optical enantiomers of the diastereomeric benzo[*a*]pyrene 7,8-diol-9,10-epoxides. *Biochem. Biophys. Res. Commun.*, *77*: 1389–1396, 1977.
 4. DiGiovanni, J. Multistage carcinogenesis in mouse skin. *Pharmacol. Ther.*, *54*: 63–128, 1992.
 5. Slaga, T. J., Bracken, W. J., Gleason, G., Levin, W., Yagi, H., Jerina, D. M., and Conley, A. H. Marked differences in the skin tumor-initiating activities of the optical enantiomers of the diastereomeric benzo[*a*]pyrene 7,8-diol-9,10-epoxides. *Cancer Res.*, *39*: 67–71, 1979.
 6. Buening, M. K., Wislocki, P. G., Levin, W., Yagi, H., Thakker, D. R., Akagi, H., Koreeda, M., Jerina, D. M., and Conney, A. H. Tumorigenicity of the optical enantiomers of the diastereoisomeric benzo[*a*]pyrene-7,8-diol-9,10-epoxides in newborn mice: exceptional activity of (+)-7 β ,8 α -dihydroxy-9 α ,10 α -epoxy-7,8,9,10-tetrahydrobenzo[*a*]pyrene. *Proc. Natl. Acad. Sci. USA*, *75*: 5358–5361, 1978.
 7. Slaga, T. J., and Fischer, S. M. Strain differences and solvent effects in mouse skin carcinogenesis experiments using carcinogens, tumor initiators and promoters. *Prog. Exp. Tumor Res.*, *26*: 85–109, 1983.
 8. Levin, W., Wood, A. W., Yagi, H., Jerina, D. M., and Conney, A. H. (\pm)-*trans*-7,8-dihydroxy-7,8-dihydrobenzo[*a*]pyrene: a potent skin carcinogen when applied topically to mice. *Proc. Natl. Acad. Sci. USA*, *73*: 3867–3871, 1976.
 9. Bresnik, E., McDonald, T. F., Yagi, H., Jerina, D. M., Levin, W., Wood, A. W., and Conney, A. H. Epidermal hyperplasia after topical application of benzo[*a*]pyrene, benzo[*a*]pyrene diol epoxides, and other metabolites. *Cancer Res.*, *37*: 984–990, 1977.
 10. Levin, W., Wood, A. W., Wislocki, P. G., Kapitulnik, J., Yagi, H., Jerina, D. M., and Conney, A. H. Carcinogenicity of benzo-ring derivatives of benzo[*a*]pyrene on mouse skin. *Cancer Res.*, *37*: 3356–3361, 1977.
 11. Kouri, R. E., Wood, A. W., Levin, W., Rude, T. H., Yagi, H., Mah, H. D., Jerina, D. M., and Conney, A. H. Carcinogenicity of benzo[*a*]pyrene and thirteen of its derivatives in C3H/10T mice. *J. Natl. Cancer Inst.*, *64*: 617–623, 1980.
 12. Cooper, C. S., Grover, P. L., and Sims, P. The metabolism and activation of benzo[*a*]pyrene. *Prog. Drug Metab.*, *7*: 295–396, 1983.
 13. Hall, M., Forrester, L. M., Parker, D. K., Grover, P. L., and Wolf, R. C. Relative contribution of various forms of cytochrome P450 to the metabolism of benzo[*a*]pyrene by human liver microsomes. *Carcinogenesis (Lond.)*, *10*: 1815–1821, 1989.
 14. Hall, M., and Grover, P. L. Stereoselective aspects of the metabolic activation of benzo[*a*]pyrene by human skin *in vitro*. *Chem.-Biol. Interact.*, *64*: 281–296, 1988.
 15. Day, B. W., Doxtader, M. M., Rich, R. H., Skipper, P. L., Singh, K., Dasari, R. R., and Tannenbaum, S. R. Human serum albumin-benzo[*a*]pyrene anti-diol epoxide adduct structure elucidation by fluorescence line narrowing spectroscopy. *Chem. Res. Toxicol.*, *5*: 71–76, 1992.
 16. Day, B. W., Skipper, P. L., Zaia, J., and Tannenbaum, S. R. Benzo[*a*]pyrene anti-diol epoxide covalently modifies human serum albumin carboxylate side chains and imidazole side chain of histidine¹⁴⁶. *J. Am. Chem. Soc.*, *113*: 8505–8509, 1991.
 17. Brunmark, P., Harriman, S., Skipper, P. L., Wishnok, J. S., Amin, S., and Tannenbaum, S. R. Identification of subdomain IB in human serum albumin as a major binding site for polycyclic aromatic hydrocarbon epoxides. *Chem.-Res. Toxicol.*, *10*: 880–886, 1997.
 18. Day, B. W., Skipper, P. L., Zaia, J., Singh, K., and Tannenbaum, S. R. Enantiospecificity of covalent adduct formation by benzo[*a*]pyrene anti-diol epoxide with human serum albumin. *Chem.-Res. Toxicol.*, *7*: 829–835, 1994.
 19. Pastorelli, R., Restano, J., Guanci, M., Maramonte, M., Magagnotti, C., Allevi, R., Lauri, D., Fanelli, R., and Airoidi, L. Hemoglobin adducts of benzo[*a*]pyrene in newspaper vendors: association with traffic exhaust. *Carcinogenesis (Lond.)*, *17*: 2389–2394, 1996.
 20. Taghizadeh, K., and Skipper, P. L. Benzo[*a*]pyrene diol epoxide and related polynuclear aromatic hydrocarbon adducts of hemoglobin. *In: J. Everse, K. D. Vandegriff, and R. M. Winslow (eds.), Hemoglobins, Part B, Methods in Enzymology*, pp. 668–674, San Diego: Academic Press, 1994.
 21. Pastorelli, R., Guanci, M., Cerri, A., Negri, E., Vecchia, C. L., Fumagalli, F., Mezzetti, M., Cappelli, R., Panigalli, T., Fanelli, R., and Airoidi, L. Impact of inherited polymorphisms in glutathione *S*-transferase M1, microsomal epoxide hydrolase, cytochrome P450 enzymes on DNA, and blood protein adducts of benzo[*a*]pyrene-diolepoxide. *Cancer Epidemiol. Biomark. Prev.*, *7*: 703–709, 1998.
 22. Nikolaou, K., Masclat, P., and Mouvier, G. Sources and chemical reactivity of polycyclic aromatic hydrocarbons in the atmosphere: a critical review. *Sci. Total Environ.*, *32*: 103–131, 1984.
 23. Santella, R. M., Lin, C. D., Cleveland, W. L., and Weinstein, I. B. Monoclonal antibodies to DNA modified by a benzo[*a*]pyrene diol epoxide. *Carcinogenesis (Lond.)*, *9*: 1773–1777, 1984.
 24. Cortes, H. J., Pfeiffer, C. D., Richter, B. E., and Stevens, T. S. Porous ceramic bed supports for fused silica packed capillary columns used in liquid chromatography. *J. High Resolution Chromatogr. Chromatogr. Commun.*, *10*: 446–450, 1987.
 25. Snedecor, G. W., and Cochran, W. G. *Statistical Methods, The Sixth Edition*. Ames, Iowa: The Iowa State University Press, 1967.
 26. Harriman, S. P., Wishnok, J. S., Skipper, P. L., and Tannenbaum, S. R. Identification and quantification of PAH-diol-epoxide adducts from enzymatic digests of HSA isolated from human plasma. *Proc. Am. Assoc. Cancer Res.*, *38*: 463, 1997.
 27. Phillips, D. H., Schoket, B., Hewer, A., Bailey, E., Kostic, S., and Vincze, I. Influence of cigarette smoking on the levels of DNA adducts in human bronchial epithelium and white blood cells. *Int. J. Cancer*, *46*: 569–575, 1990.
 28. Dunn, B. P., Vedal, S., San, R. H. C., Kwan, W. F., Nelems, B., Enardson, D. A., and Stitch, H. F. DNA adducts in bronchial brush biopsies. *Int. J. Cancer*, *48*: 485–492, 1991.
 29. Yoshimoto, M., Okuno, S., Yoshinaga, M., Yamakawa, O., Yamaguchi, M., and Yamada, J. Antimutagenicity of sweet potato (*Ipomoea batatas*) roots. *Biosci. Biotech. Biochem.*, *63*: 537–541, 1999.
 30. Dakovic-Svajcer, K., Samojlik, I., Raskovic, A., Popovic, M., and Jakovljevic, V. The activity of liver oxidative enzymes after single and multiple grapefruit juice ingestion. *Exp. Toxicol. Pathol.*, *51*: 304–308, 1999.
 31. Dubowsky, S. K., Wallace, L. A., and Buckley, T. J. The contribution of traffic to indoor concentrations of polyaromatic hydrocarbons. *J. Expo. Anal. Environ. Epidemiol.*, *9*: 312–321, 1999.